DOI: 10.24850/j-tyca-2026-01-10

Articles

Assessment of chlorophyll indices with Sentinel-2 data in San Roque reservoir, Córdoba, Argentina

Valoración de índices de clorofila con datos Sentinel-2 en el embalse San Roque, Córdoba, Argentina

Mariana Pagot[1], ORCID: https://orcid.org/0000-0002-7435-3381

María Inés Rodriguez[2], ORCID: https://orcid.org/0000-0002-2649-4841

Micaela Juaneda[3], ORCID: https://orcid.org/0009-0000-5152-219X

Araceli Ferreyra[4], ORCID: https://orcid.org/0009-0006-5855-9677

Marcelo Smrekar[5], ORCID: https://orcid.org/0000-0002-7043-8134

Andrés Rodriguez[6], ORCID: https://orcid.org/0000-0002-4110-6464

[1]Laboratorio de Hidráulica, Facultad de Ciencias Exactas, Físicas y Naturales, Universidad Nacional de Córdoba, Córdoba, Argentina, mariana.pagot@unc.edu.ar

[2]Instituto Nacional de Agua, delegación Centro de Investigación de la Región Semiárida, Córdoba, Argentina, minesrodrig@gmail.com

[3]Laboratorio de Hidrometeorología, Facultad de Ciencias Exactas, Físicas y Naturales, Universidad Nacional de Córdoba, Córdoba, Argentina, micajuaneda@mi.unc.edu.ar

[4]Laboratorio de Hidrometeorología, Facultad de Ciencias Exactas, Físicas y Naturales, Universidad Nacional de Córdoba, Córdoba, Argentina, araceli.ferreyra@mi.unc.edu.ar

[5]Laboratorio de Hidrometeorología, Facultad de Ciencias Exactas, Físicas y Naturales, Universidad Nacional de Córdoba, Córdoba, Argentina, marcelo.smrekar@unc.edu.ar

[6]Laboratorio de Hidráulica / Laboratorio de Hidrometeorología, Facultad de Ciencias Exactas, Físicas y Naturales, Universidad Nacional de Córdoba, Córdoba, Argentina, andres.rodriguez@unc.edu.ar

Corresponding author: Mariana Pagot, mariana.pagot@unc.edu.ar

Abstract

In this study, specific indices derived from Sentinel-2, processed using Google Earth Engine (GEE), were used to estimate chlorophyll-a (Chl-a) concentration in the San Roque Reservoir, Córdoba, Argentina. The evaluated indices include the normalized difference chlorophyll index (NDCI), normalized difference vegetation index (NDVI), green chlorophyll index (GCI), and red chlorophyll index (RCl).

The NDCI index resulted the best option among the four specific indexes evaluated, providing a fit with a coefficient of determination (R^2) close to 0.8 and statistically significant in relation to measured Chl-a values. It accurately represents the spatial and temporal dynamics of the measured Chl-a concentrations. The application of this index would improve the current management tools for this important provincial water body.

Keywords: Sentinel-2, Chlorophyll-a, Chl-a, NDCI, NDVI, GCI, RCl, GEE, San Roque reservoir, Argentina.

Resumen

En este estudio se utilizaron índices específicos con productos de Sentinel-2, procesados con *Google Earth Engine* (GEE), para estimar la concentración de clorofila-a (Cl-a) en el embalse San Roque, Córdoba, Argentina. Los índices específicos evaluados fueron el índice de clorofila de diferencia normalizada (NDCI), índice de vegetación de diferencia normalizada (NDVI), índice de clorofila en banda verde (GCI) e índice de clorofila en banda roja (RCl).

El índice NDCI ha demostrado ser la mejor opción entre los cuatro índices específicos evaluados, al proporcionar un ajuste con coeficiente de determinación (R^2) cercano a 0.8 y estadísticamente significativo respecto a valores medidos de Cl-a, y que representa de forma adecuada la dinámica espacial y temporal de los valores medidos de Cl-a. Aplicar este índice significaría mejoras en las herramientas de gestiones actuales para este importante cuerpo de agua provincial.

Palabras clave: Sentinel-2, Clorofila-a, Cl-a, NDCI, NDVI, GCI, RCl, GEE, embalse San Roque, Argentina.

Received: 27/02/2025

Accepted: 28/05/2025

Available ahead of print: 25/06/2025

Version of record: 01/01/2026

Introduction

Freshwater bodies are important sources of drinking water, especially in semi-arid regions, such as central Argentina. The presence of algal blooms in water degrades its quality for both human and agricultural consumption, as well as for recreational purposes. The eutrophication of reservoirs exerts harmful pressure on the aquatic ecosystem involved (Li & Li, 2024).

Remote sensing is an effective complement to field sampling methods, as it allows data to be collected from very large areas (Li & Li, 2004; Chawla, Karthikeyan, & Mishra, 2020) and smaller ones, such as the San Roque Reservoir, in the province of Córdoba. Numerous studies have achieved successful results through satellite image processing and numerical correlation of electromagnetic spectrum ranges with the temporal and spatial distribution of water quality variables, including: Richardson (1996); Bazán *et al*. (2005); Pagot, Rodriguez, Hillman, Corral and Niencheski (2007); Gitelson *et al*. (2008); Gilerson *et al*. (2010); Palmer *et al*. (2015); Yu, Bai, He, Gong and Li (2023), and Li, Hao, Wu and Nie (2024).

In particular, Sentinel-2 products have been used for estimating suspended particle concentrations (Liu *et al*., 2017), chlorophyll-a (Chl-a) concentrations in small reservoirs in Ambrose-Igho (2019); Maier & Keller (2019); Xu *et al*. (2019); Caballero and Navarro (2021); German, Shimoni, Beltramone and Rodríguez (2021); Bramich, Bolch and Fischer (2021); Kislik, Dronova, Grantham and Kelly (2022); Barraza-Moraga, Alcayaga, Pizarro, Félez-Bernal and Urrutia (2022), among other quality parameters.

This study includes monthly monitoring of the water quality of the San Roque Reservoir using conventional sampling methods carried out by the Instituto Nacional del Agua (INA) through its delegation, Centro de Investigación de la Región Semiárida (CIRSA) in Córdoba, Argentina.

The aim of this work is to apply specific indices with Sentinel-2 products to estimate the Chl-a concentration in the San Roque Reservoir and analyze the fit of these satellite indices with laboratory-measured values obtained from collected samples.

Materials y methods

Area of interest

The area of interest is located in the San Roque Reservoir, in the province of Córdoba, central region of Argentina (Figure 1). The geographic coordinates (latitude, longitude) of the reservoir's center are: 31.38° S, 64.47° W. This small reservoir, with a maximum depth of 35.3 m, supplies drinking water to two-thirds of the population of Córdoba city (1.3 million of habitants), the second most populous city in Argentina. The water surface area is 15 km², with a catchment area of 1750 km². The reservoir is located in a semi-arid temperate region with an average annual temperature of 17 °C and an average annual precipitation of 720 mm. Numerical modeling of this reservoir has recently been developed by Ponce, Rodríguez, Ruibal-Conti, Muchiut and Rodríguez (2023), and Muchiut, Rodríguez, Ruibal-Conti, Ruiz and Rodriguez (2024).

Tecnología y Ciencias del Agua
OPEN ACCESS
Check for updates

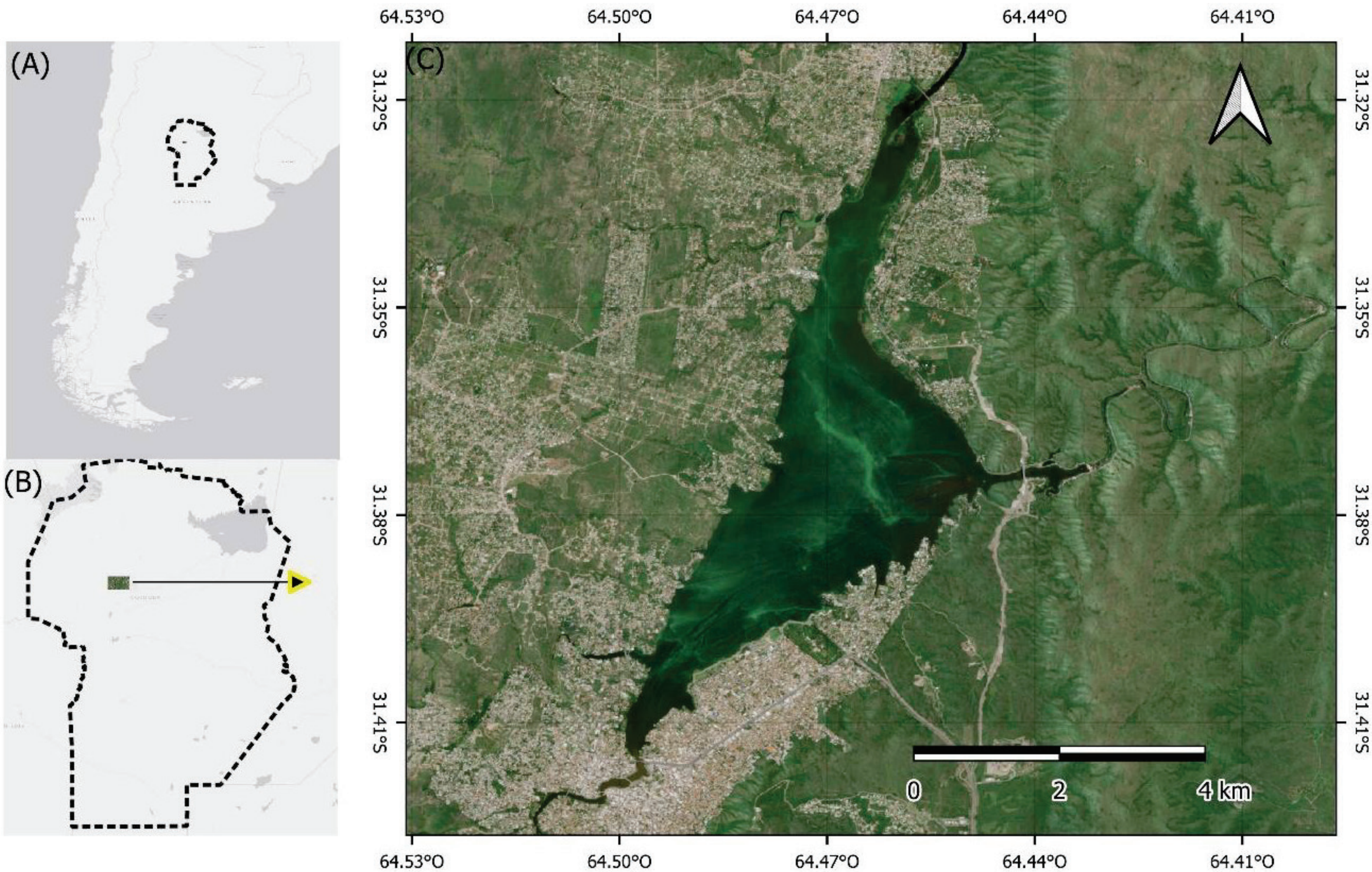

Figure 1. Area of the study. Sentinel-2 image of the San Roque Reservoir. Algal blooms during February 18, 2022 (green color within the water body). Bands 4-3-2 (R-G-B).

Description of the specific indices used

The following four spectral indices were selected to calibrate the Chl-a algorithms in the San Roque Reservoir using Sentinel-2 images, based on the monitoring data available between 2021 and 2024.

1. NDCI (Normalized Difference Chlorophyll Index): Uses the spectral range between wavelengths 650 nm and 713 nm. It is useful and practical to apply to areas with phytoplankton-rich waters (Mishra & Mishra, 2012).

2. NDVI (Normalized Difference Vegetation Index): A simple indicator of photosynthetically active biomass, calculated from the ratio between near-infrared (NIR) and red (RED) reflectances of the electromagnetic spectrum. This index is used worldwide in vegetation monitoring (Gilabert, González-Piqueras, & García-Haro, 1997).

3. GCI (Green Chlorophyll Index): Calculated as the ratio of the reflectance of chlorophyll in the near-infrared (NIR) band to the reflectance in the green band (GREEN). It is intended for bodies of water with moderate concentrations of chlorophyll (Gitelson & Yacobi, 1995).

4. RCI (Chlorophyll Red Index): Calculated as the ratio of the reflectance of chlorophyll in the near infrared band 8A (NIR_narrow) to the reflectance in the red band (RED) (Ha, Thao, Koike, & Nhuan, 2017).

The mathematical expressions used are presented in Table 1.

Table 1. Specific indices used for the estimation of Chl-a

Method	General expression	Sentinel-2 expression	Source
(1) NDCI	$\frac{(RED_{EDGE} - RED)}{(RED_{EDGE} + RED)}$	$\frac{(B05 - B04)}{(B05 + B04)}$	Mishra and Mishra (2012)
(2) NDVI	$\frac{(NIR - RED)}{(NIR + RED)}$	$\frac{(B08 - B04)}{(B08 + B04)}$	Gilabert *et al*. (1997
(3) GCI	$\frac{(NIR)}{(GREEN)}$	$\frac{B08}{B03}$	Gitelson and Yacobi, (1995), and Ha *et al*. (2017)
(4) RCI	$\frac{(NIR_{Narrow})}{(RED)}$	$\frac{B08A}{B04}$	Ha *et al*. (2017)

Data *in situ*

For more than 25 years, INA-CIRSA has carried out monthly monitoring of the San Roque Reservoir in the province of Córdoba, whose outfall is the Suquía River, a tributary of the Mar Chiquita Lagoon (the largest endorheic salt lagoon in South America). CIRSA collects and publishes both hydrometeorological and water quality data from the reservoir. Water quality samples were collected at four (4) monitoring stations (Figure 2) defined as follows: center of the reservoir "Station C" (31.38° S, 64.46° W); next to the water intake "Station TAC" (31.37° S, 64.43° W); Cosquín Outflow "Station DCQ" (31.32° S, 64.46° W) and San Antonio Outflow "Station DSA" (31.41° S, 64.49° W).

Tecnología y Ciencias del Agua
OPEN ACCESS
Check for updates

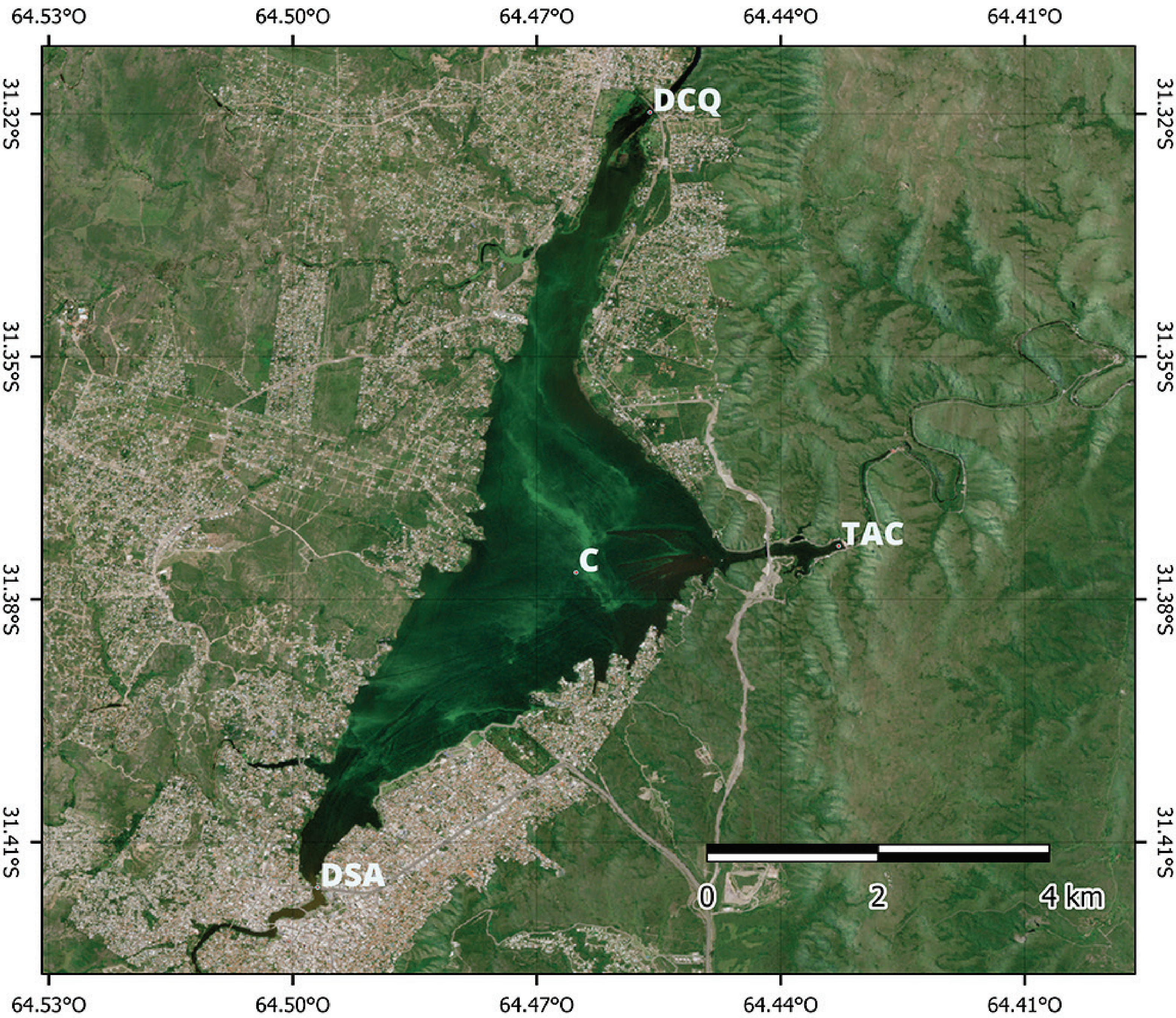

Figure 2. Monitoring stations at the San Roque Reservoir. References: C (center); TAC (Water Intake); DCQ (Cosquín Outflow); and DSA (San Antonio Outflow).

Tecnología y Ciencias del Agua
OPEN ACCESS
Check for updates

The available database covers the period from 1999 to 2024 with a monthly interval. These data included Chl-a concentrations (in μg/l), measured from water samples collected at different depths (0.2, 1.0, 1.5, and 2.0 m) taken within the interval of 9:00 to 12:00 a.m., and subsequently analyzed in the laboratory, according to GEMS/WATER regulations (GEMS/WATER, 1992). The study period covered the years 2021 and 2024. The available Chl-a data for each monitoring station (Figure 2) are presented in Figure 3. These data were statistically processed, considering as outliers those values greater than two interquartile ranges of the third quartile.

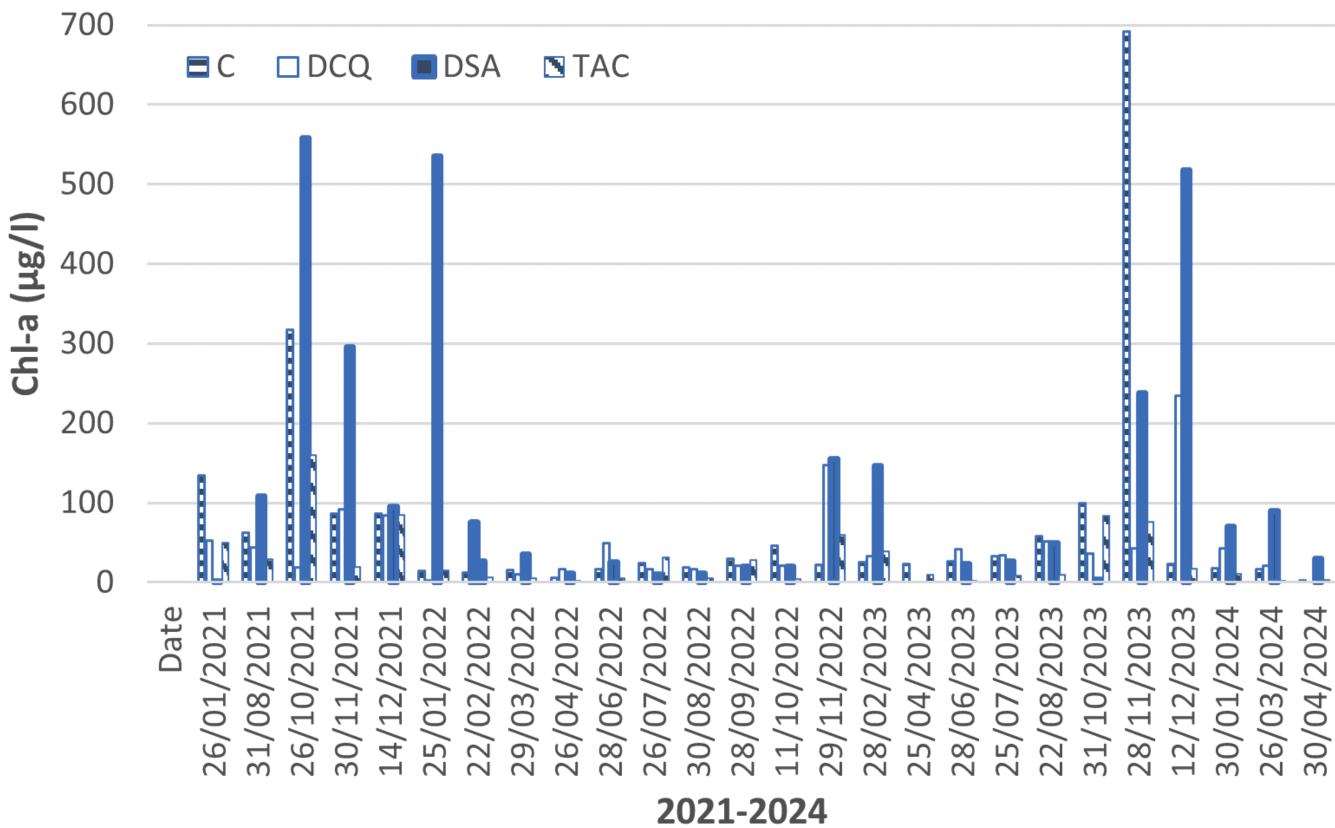

Figure 3. Chl-a recorded with measurements at monitoring stations. Source: INA-CIRSA (2024).

Satellite data: Sentinel-2 image collection and processing

The Sentinel-2 mission, part of the European Space Agency's (ESA) Copernicus Earth Observation program, consists of polar-orbiting satellites (S2A and S2B) that provide optical images. These images have a spatial resolution of 10 to 20 m, depending on the spectral band, with 5 days of temporal resolution. By combining data from S2A and S2B, a revisit interval of approximately 2 days is achieved over the study area. These satellites captured information on the scene that includes the San Roque Reservoir at approximately 11:30 a.m., coinciding with the time window of the in situ sampling.

Level 2A imagery processing with cartographic geometry (UTM/WGS84 projection) was used, providing Surface Reflectance (SR) products with bottom-of-atmosphere (BOA) corrections. These products, as well as the Surface Reflectance for the different spectral bands, are resampled at different spatial resolutions. The characteristics of the spectral bands used are presented in Table 2 (ESA, 2025).

Table 2. Spectral band configuration for Sentinel-2.

Band	**Designation**	**Spectral range / central wavelength (nm)**	**Spatial resolution (m)**
3	Green	543–578/560	10
4	Red	650–680/665	10
5	Red Edge	698–713/705	20
8	Near Infrared (NIR)	785–900/842	10
8A	NIR_narrow	855–875/865	20

Source: ESA (2025).

Tecnología y Ciencias del Agua

Google Earth Engine for processing Sentinel-2 images

The Google Earth Engine-GEE program (GEE, 2022) was used, which allows analysis of the collected satellite images through a programming interface. A custom script was developed to perform the following steps:

1. Define the monitoring stations as points of interest (C, TAC, DCQ, DSA) with their respective coordinates
2. Define the monitoring dates for the period 2021-2024
3. Collect Sentinel-2 images that coincide with or differ by a maximum of 4 days from the defined dates
4. Create a 20 m buffer at each point of interest and calculate the programmed indices (NDCI, NDVI, GCI and RCI) for each image in the collected Sentinel-2 collection
5. Extract the spectral band values and calculated indices into a *.CSV file
6. Visualize the results

The flow diagram describing the methodology used to determine Chl-a concentration with satellite data is presented in Figure 4.

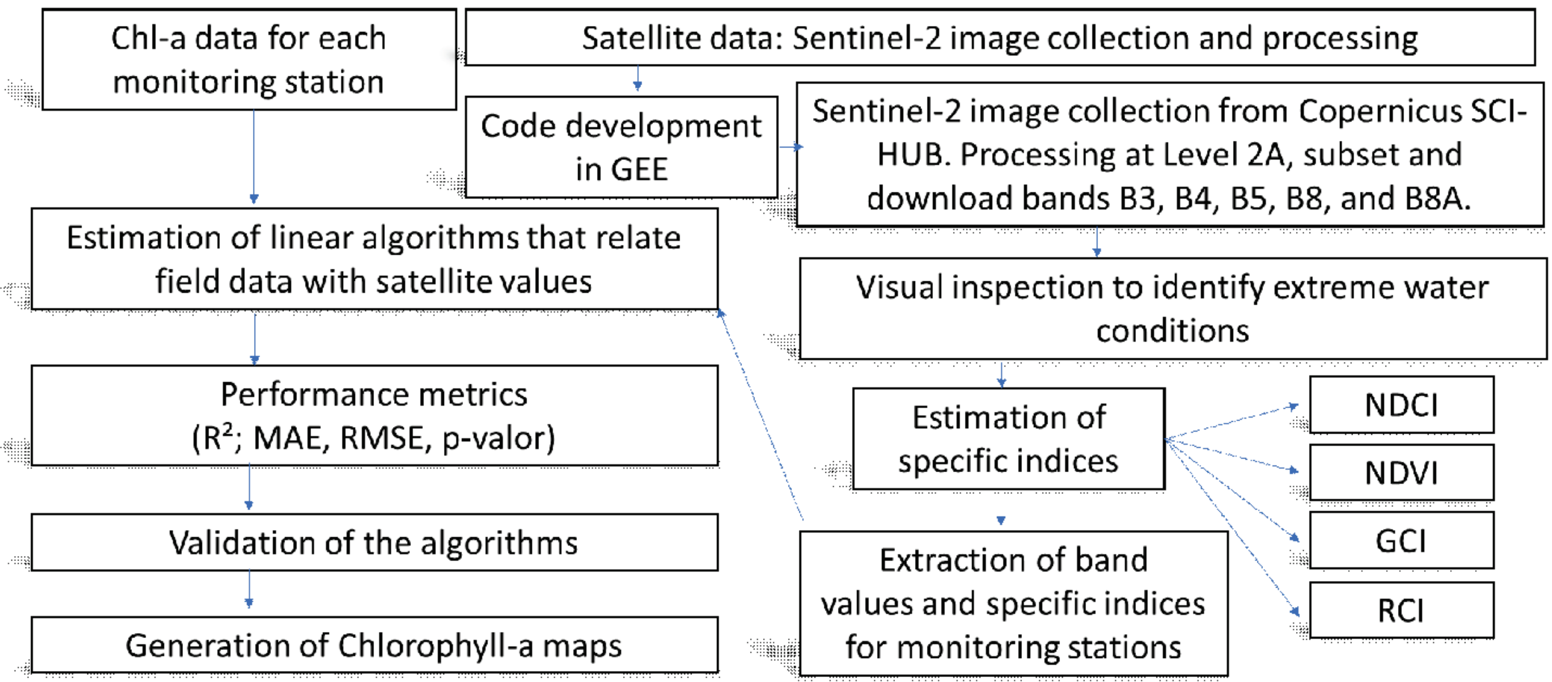

Figure 4. Flow diagram for the methodology used to determine Chl-a values with satellite data.

Performance metrics

To identify the best relationship between the measured Chl-a data and the corresponding values estimated with the satellite algorithms for each specific index, the performance metrics listed in Table 3 were evaluated for each function: the coefficient of determination (R^2), the mean absolute error (MAE), the root mean square error (RMSE) and the probability under the null hypothesis (*p*-valor) (Legates & McCabe, 1999; Wackerly, Mendenhall III, & Scheaffer, 2008).

Table 3. Performance metrics used.

Metric	Symbol	General expression	Observation
Coefficient of determination	R^2	$1-\frac{\sum_{i=1}^{n}\ (yi-xi)^2}{\sum_{i=1}^{n}\ \left(yi-\underline{y}\right)^2}$ (5)	Describes the proportion of the total variance in the observed data that the model can explain. It ranges from 0 to 1.0; higher values indicate better fit
Mean absolute error	MAE	$\frac{\sum_{i=1}^{n}\ \lvert yi-xi\rvert}{n}$ (6)	It is the difference between the estimated value and the actual value at each estimated point
Root mean square error	RMSE	$\sqrt{\frac{\sum_{i=1}^{n}\ (yi-xi)^2}{n}}$ (7)	It measures the average magnitude of the errors. The lower the RMSE, the better the model and its estimates
Probability under the null hypothesis	*p*-valor	$p=2min\{Pr\ Pr\ (T\geq t\lvert HO)\ ,Pr(\lvert T\rvert\leq t\lvert HO)\}$ (8)	Probability under the null hypothesis of obtaining a true-valued test statistic at least as extreme as the one obtained

Xi = estimated Chl-a concentration values

Yi = measured Chl-a data

N = Number of observations

The p-value parameter considers an observed test statistic t of unknown T distribution; p-value is the probability of observing a test statistic value at least as extreme as t if the null hypothesis Ho were true

Results

A total of twenty-three Sentinel-2 multispectral images were collected between 2021 and 2024 for the study area, covering the defined sampling sites using a 20 m diameter buffer (defined based on the maximum pixel size used), with a maximum interval of 4 days around the available *in-situ* monitoring dates. In this dataset, 87 % of the images were acquired within 0 and 2 days of the monitoring date (0 days: 37 %; 1 day: 20 %; 2 days: 30 %, and between 3-4 days: 13 %).

During the analysis period, the average depth of the Cosquín River was 1.1 m, with extreme values ranging from 0.7 m (minimum) to 6.6 m (maximum). In the case of the San Antonio River, significantly more variable depths were recorded, with an average depth of 0.5 m, a minimum of 0.1 m, and a maximum of 13.3 m. For this period, the average water depth in the San Roque Reservoir was 33 m, with minimum values of 28.4 m and maximum of 36.7 m. Due to the low water levels recorded simultaneously in both the San Antonio River and the San Roque Reservoir, a detailed visual inspection of selected satellite images was performed.

The image acquired on November 29, 2022, revealed an area without water coverage at the mouth of the San Antonio River (Figure 5, Left). This retraction of the water body is associated with a water depth of 0.2 m in the San Antonio River and a level with respect to the bed in the reservoir of 29.2 m (0.8 m above the minimum recorded during the study period) (Figure 5, Right). Due to this atypical condition for the period analyzed, this image was excluded from the dataset considered in this study. This decision is in line with the consistency and temporal representativeness criteria applied in Li, Martin and Estival (2017), and

Zhang, Yuan, Zeng, Li and Wei (2018), which highlight the importance of using images that reflect representative conditions to avoid bias in the analysis.

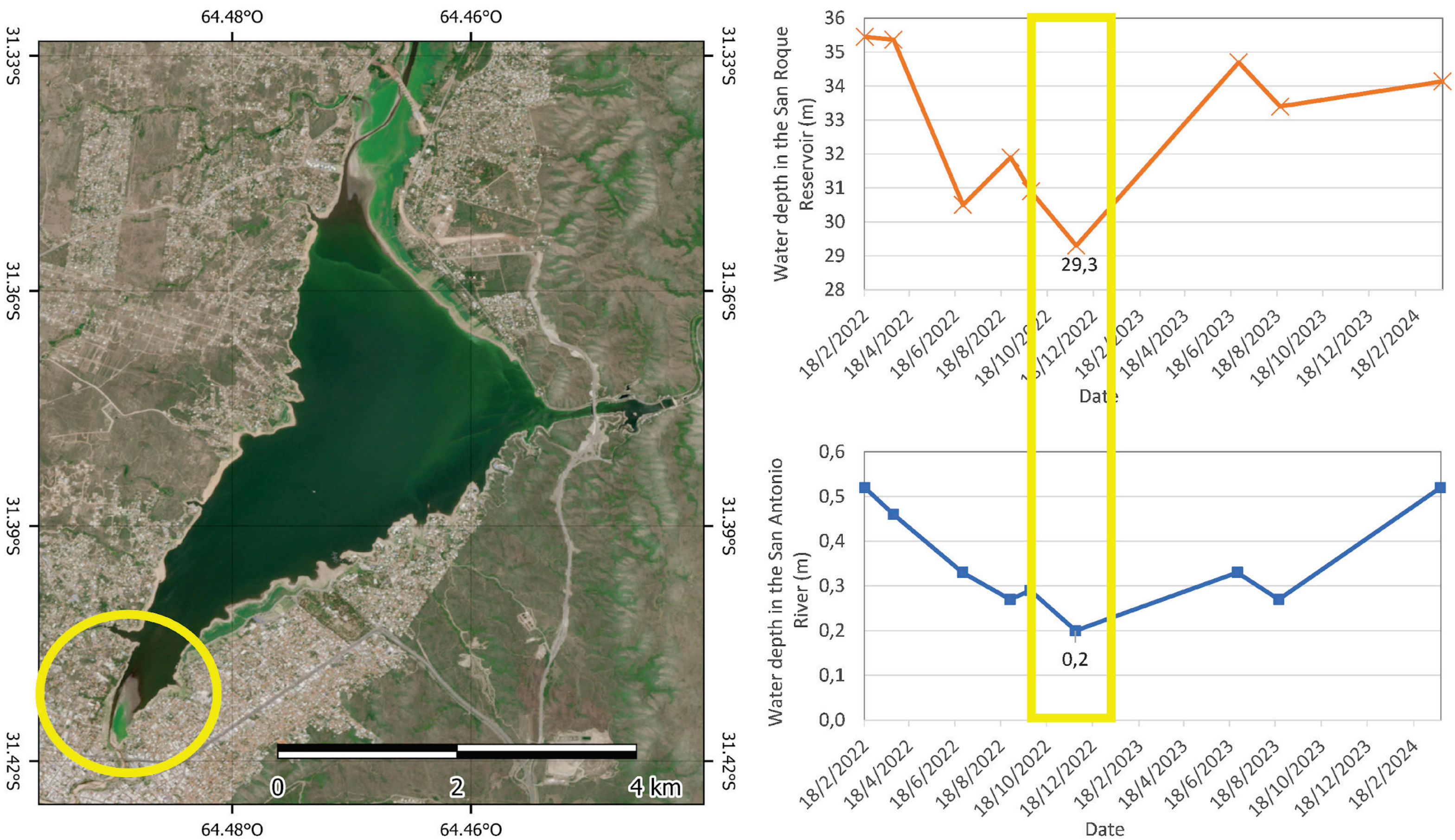

Figure 5. (Left) Sentinel-2 image from 2022-11-29 (yellow circle: San Antonio Outflow). (Right) Water depth in: (a) San Roque Reservoir and (b) San Antonio River (yellow box associated with the date of the satellite image).

From the selected satellite images, the reflectance values for each band involved in the calculation of the specific indices were processed

(Table 1). The resulting indices for each monitoring station are presented in Figure 6.

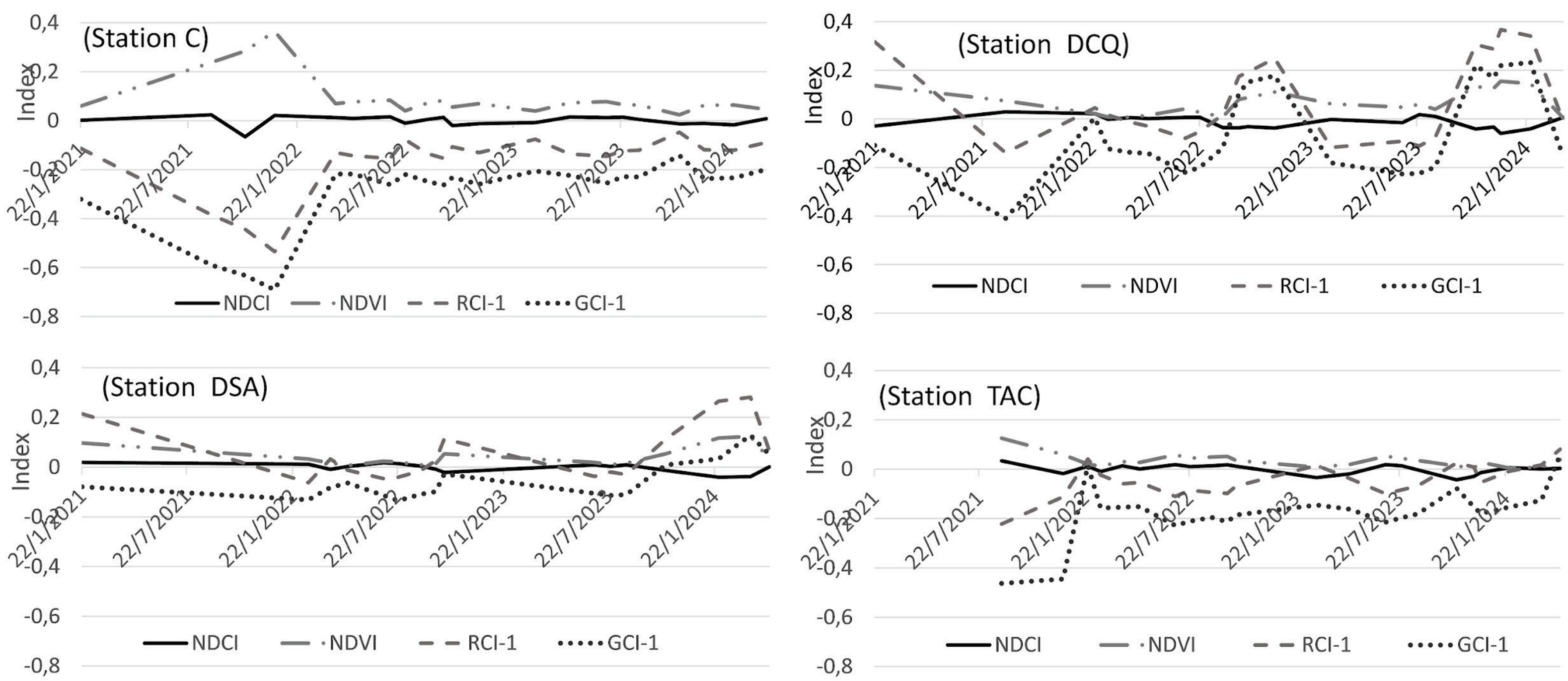

Figure 6. Specific indices estimated at each monitoring station: C, DCQ, DSA, and TAC.

Once the selected chlorophyll-a dataset was defined, the corresponding indices were estimated. Specifically, for February 18, 2022, representative maps of each specific index were generated, modeling the San Roque Reservoir area. Figure 7 presents these maps, processed using the QGIS software (QGIS.org, 2025).

Tecnología y Ciencias del Agua
OPEN ACCESS

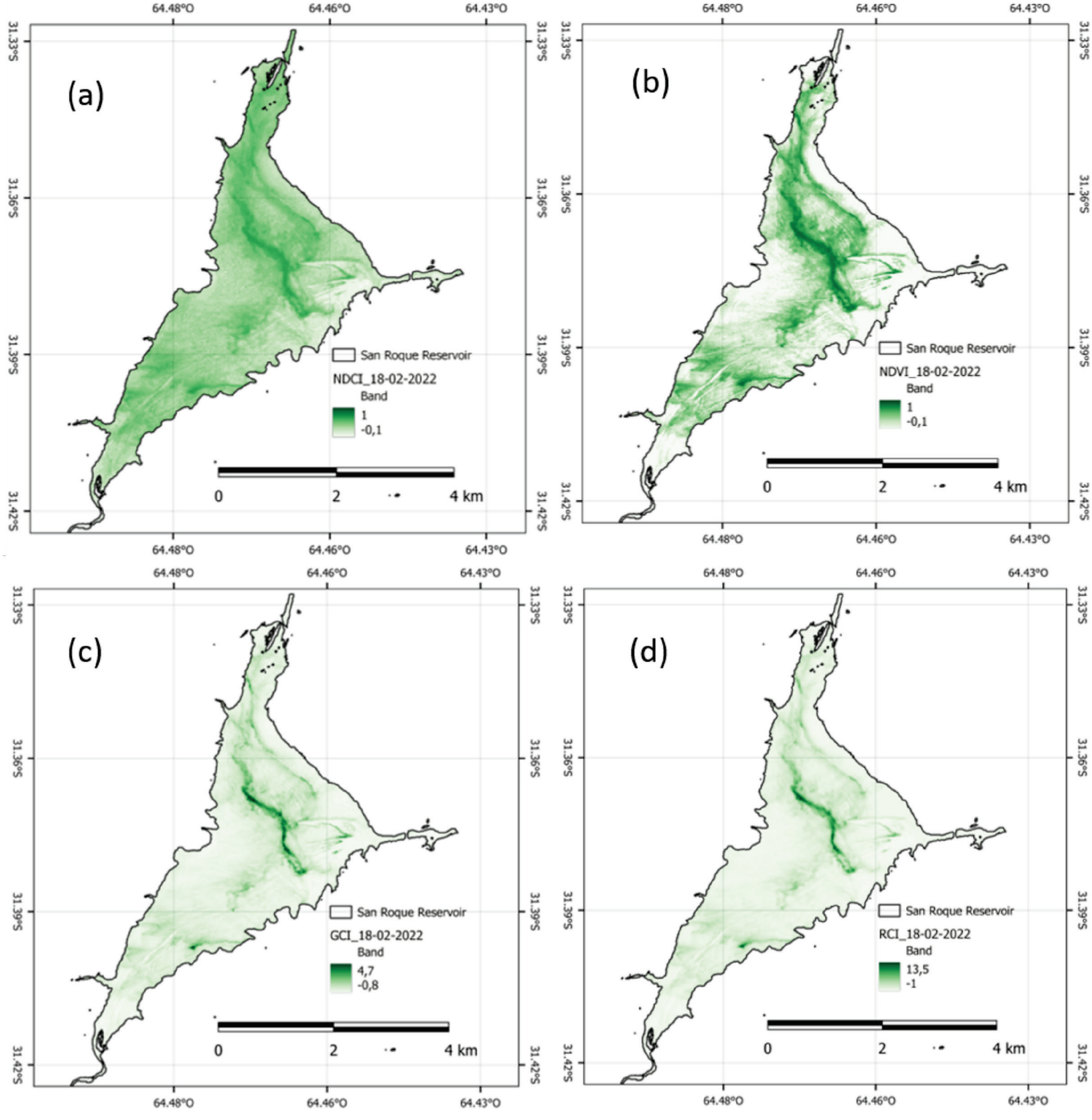

Figure 7. Modeling of specific indices for San Roque Reservoir: (a) NDCI, (b) NDVI, (c) GCI, and (d) RCI.

Two subsets used for calibration and validation were analyzed. The first subset consisted of 35 pairs of values, ranging from 2 µg/l to 235 µg/l of Chl-a. The relationships between Chl-a measurements and values of each specific index were established using a polynomial function of degree 2 through linear regression (Equation (9)), since the relationship between the specific indices (X) and the measured Chl-a values is nonlinear (y):

$$y = A + B.X + C.X^2 \tag{9}$$

Where *A*, *B*, and *C* are the coefficients to be calibrated.

Figure 8 presents the four models determined along with their corresponding coefficients of determination (R^2).

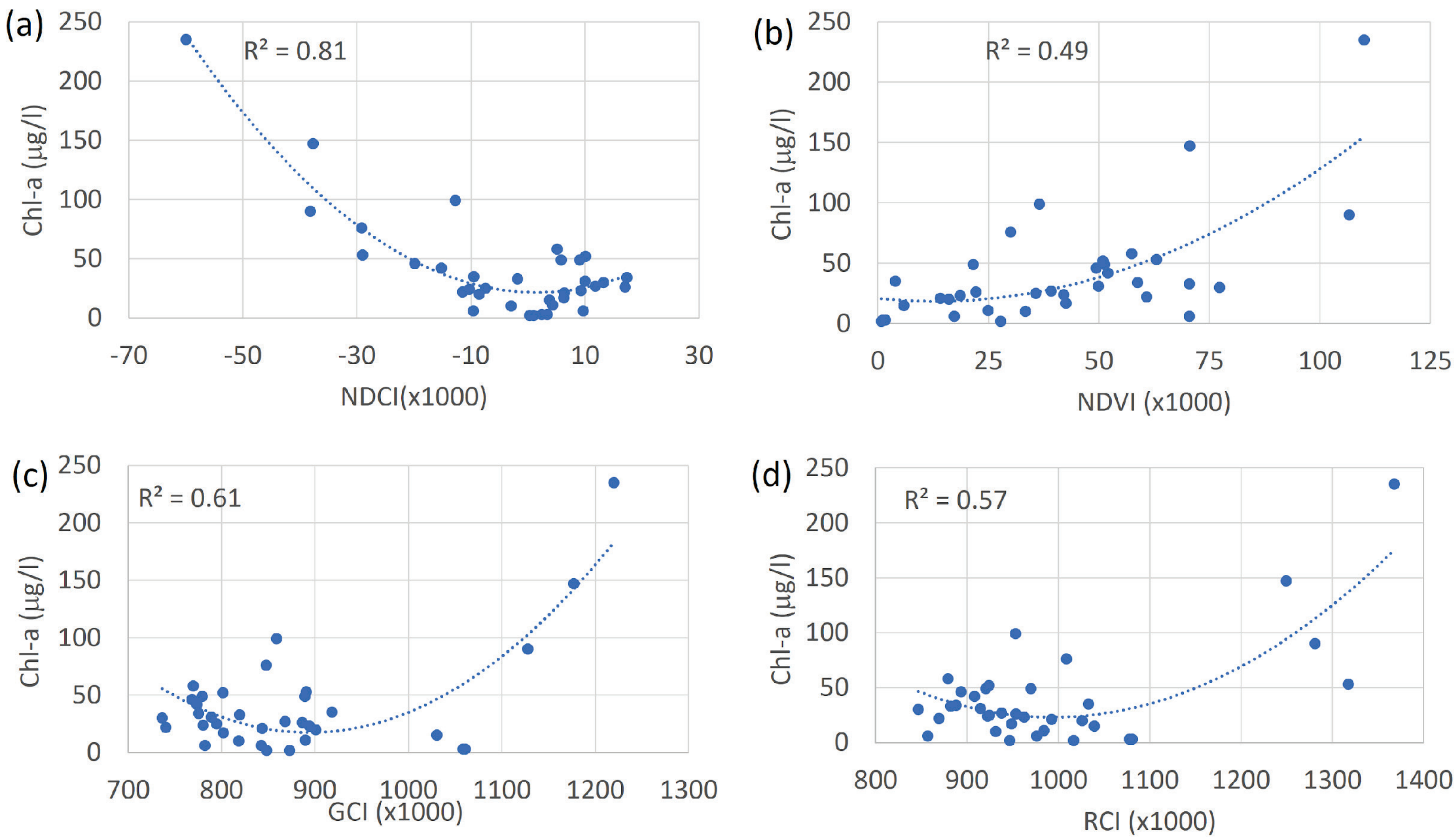

Figure 8. Specific indices based on measured values. (a) NDCI, (b) NDVI, (c) GCI, and (d) RCI. Linear regression models and coefficient of determination (R^2) con n = 35.

Discussion

The results obtained for each parameter using the performance metrics detailed in Table 3 are presented in Table 4.

Table 4. Statistical parameters between Chl-a based on specific indices and measured Chl-a.

Metric	NDCI	NDVI	GCI	RCI
R^2	0.81	0.49	0.61	0.57
MAE (µg/l)	13.9	22.1	20.8	20.9
RMSE (µg/l)	19.4	31.9	28.2	29.4
p-valor (%)	1.3e-13	2.2e-06	3.6e-08	1.4e-07

The model with the highest coefficient of determination (R^2) was the one estimated with the NDCI index (R^2 = 0.81), and the model that achieved the least fit was based on the NDVI index (R^2 = 0.49). The mean absolute error (MAE) was 13.9 µg/l for the NDCI model and close to 21 µg/l for the other models evaluated. With respect to the root mean square error, the lowest result was obtained with the NDCI index (RMSE = 19.4 µg/l), while the maximum value was obtained for the NDVI index (RMSE = 31.9 µg/l). For the four models with specific indices, a probability (*p*-value) lower than the established threshold of 0.0001 % was obtained.

Based on these results, the algorithm estimated with NDCI is considered to be the best fit, as it achieved the highest R^2 value and the lowest MAE, RMSE, and p-values compared to the other indices evaluated.

Furthermore, the width of the spectral range of the bands used could influence the estimation accuracy. Thus, band 8 (Table 2) has the greatest spectral range (115 nm) compared to the other bands used (which vary between 35 and 15 nm). This condition can be attributed to the fact that the NDVI index had the lowest coefficient of determination

(R^2) and the highest MAE, RMSE, and *p*-values compared to the other estimated indices.

Subsequently, the effectiveness of the proposed algorithm for the NDCI index was evaluated through statistical analysis of the validation set consisting of 32 pairs of Chl-a values available from monitoring and the corresponding values estimated using the selected model. As a result of the proposed linear regression (Figure 9), a correlation coefficient R^2 = 0.78 was obtained, indicating a good relationship between the variables. For this relationship, the MAE = 21 µg/l, RMSE = 33.5 µg/l, and p-value=2x10-8, lower than the limit (< 0.0001), were obtained.

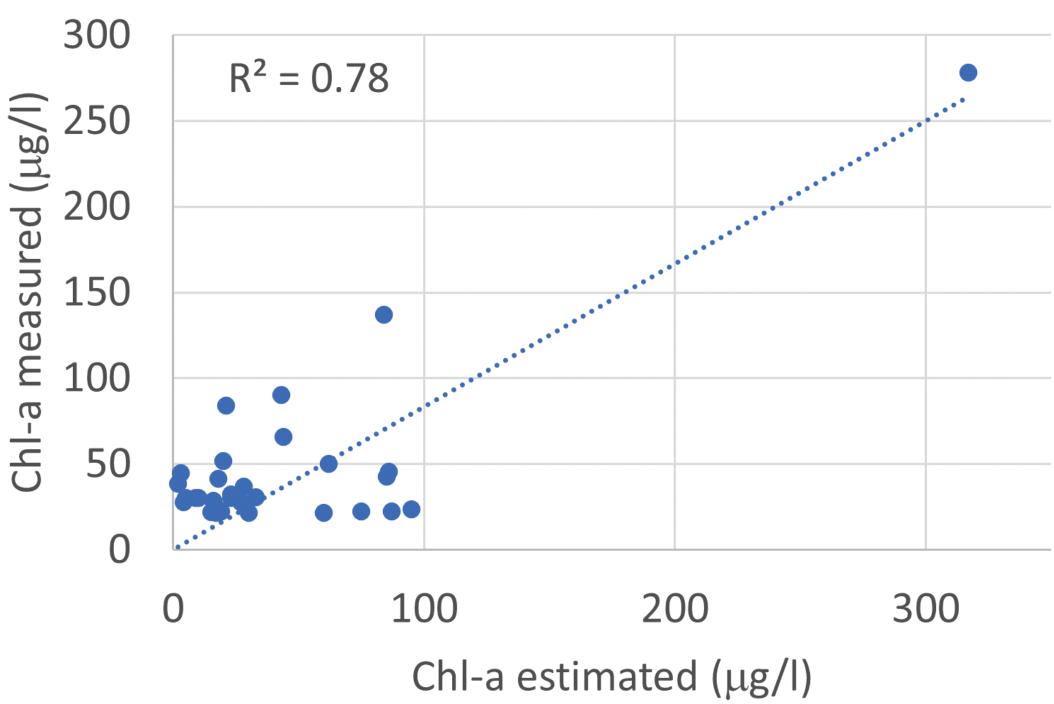

Figure 9. Measured vs. estimated Chl-a based on the NDCI index. Regression model and coefficient of determination (R^2) with n = 32.

Thus, the parameters A, B and C for Eq.9 that allow the estimation the Chl-a values based on the NDCI index are shown in Table 5.

Table 5. Calibrated parameters for the relationship NDCI and Chl-a.

Parameter (Equation (9))	Coefficient
A	21.737
B	0.178
C	0.057

The application of this algorithm to the dataset is presented in Figure 10, where measured and estimated Chl-a values are graphed as a function of the NDCI index. A good representation of the estimated values in terms of the spatial and temporal dynamics with respect to the measured values can be observed at the four monitoring stations, generally representing the temporal variability at each monitoring station (C, DCQ, DSA and TAC).

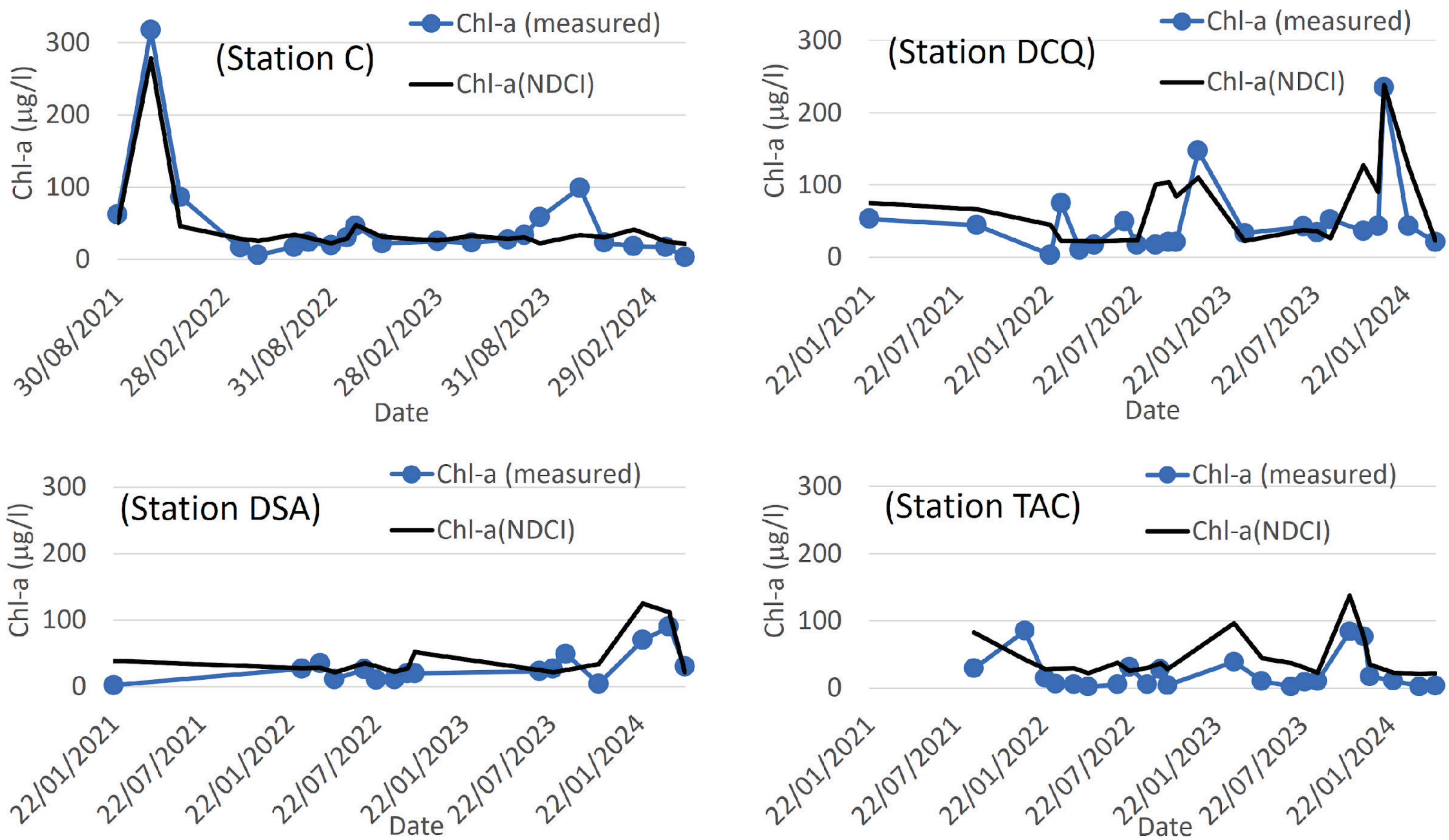

Figure 10. Measured and estimated Chl-a (based on NDCI) for each monitoring station (C, DCQ, DSA, and TAC).

Figure 11 presents a spatial distribution map of Chl-a based on the proposed modeling with the parameters defined in Table 5 for the date of February 18, 2022 in the water body of the San Roque Reservoir.

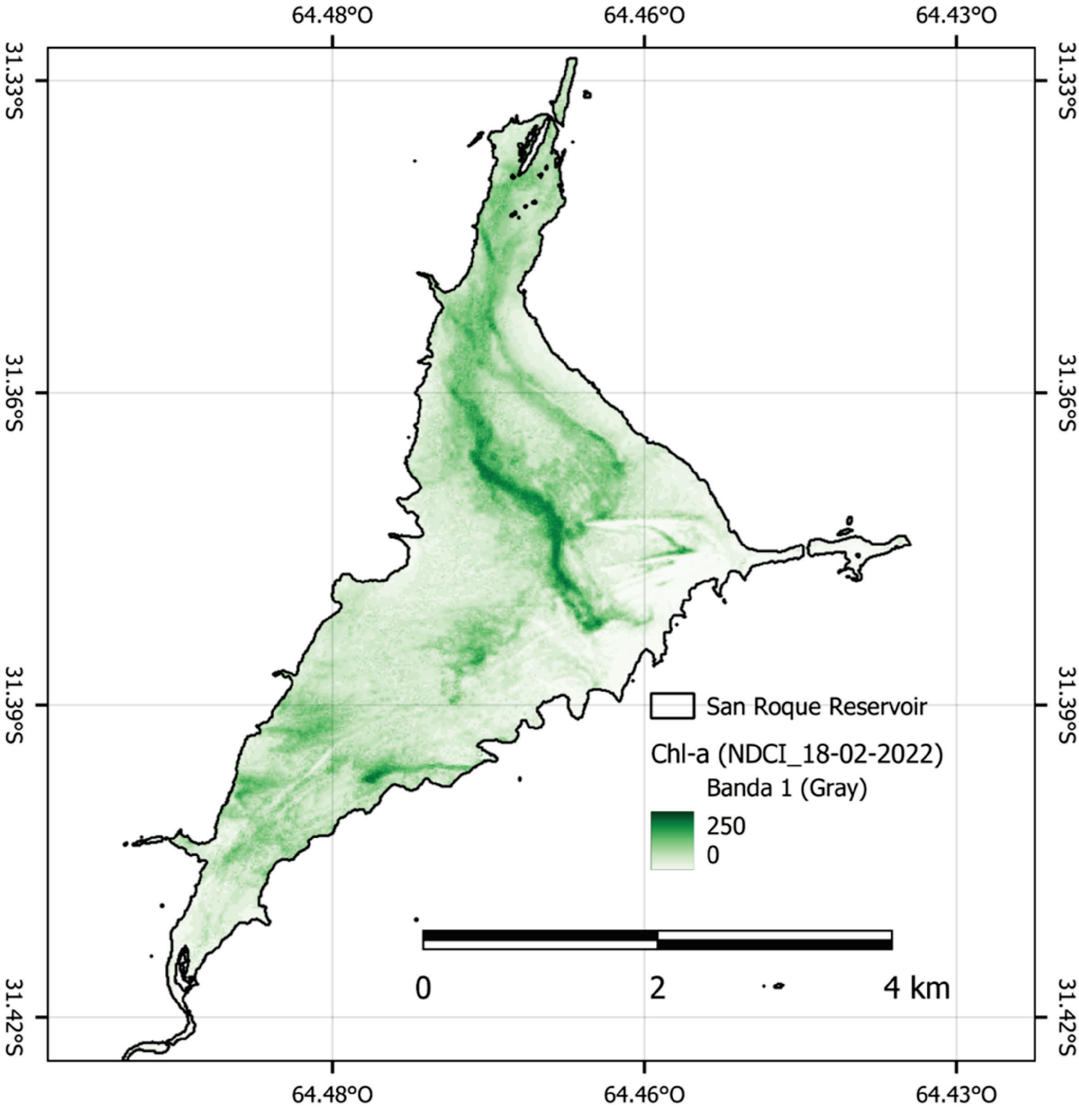
64.48°O
64.46°O
64.43°O
31.33°S
31.36°S
31.39°S
31.42°S
San Roque Reservoir
Chl-a (NDCI_18-02-2022)
Banda 1 (Gray)
250
0
0
2
4 km

Figure 11. Chl-a model (in μg/l) based on the NDCI index for the San Roque Reservoir. February 18, 2022.

Conclusions

This study utilized high-resolution satellite imagery (10–20 m) with a revisit frequency of 2–5 days from the Sentinel-2 mission, processed using the Google Earth Engine platform.

The Normalized Difference Chlorophyll Index (NDCI) has proven to be the best option among the specific indices evaluated (along with NDVI, GCl, and RCl), providing a robust fit (R^2 close to 0.8) and statistical significance. Its performance outperforms the other models analyzed here, making it suitable for application in estimating Chl-a concentrations. New functions that improve this relationship in estimating values will continue to be explored.

The proposed relationship adequately represents the spatial and temporal dynamics of the measured Chl-a concentration values at the four monitoring stations (C, DCQ, DSA, and TAC). Therefore, this satellite modeling is considered to contribute to the available tools for determining Chl-a in space and time. These results complement the monthly monitoring that has been conducted for more than 25 years at the San Roque Reservoir, due to its importance as the main source of drinking water for the second most populous city in Argentina.

Acknowledgments

Thanks to the Facultad de Ciencias Exactas, Físicas y Naturales de la Universidad Nacional de Córdoba, the Instituto Nacional del Agua, a Aguas Cordobesas and the Administración Provincial de Recursos Hídricos, province of Córdoba.

References

Ambrose-Igho, G. (2019). *Spatiotemporal analysis of lake water quality indicators on small lakes, Lake Bloomington and Evergreen Lake in* Central Illinois, using satellite remote sensing (tesis de maestría). Illinois State University, USA. Retrieved from https://ir.library.illinoisstate.edu/etd/1190

Barraza-Moraga, F., Alcayaga, H., Pizarro, A., Félez-Bernal, J. & Urrutia, R. (2022). Estimation of chlorophyll. A concentrations in Lanalhue Lake using Sentinel-2 MSI satellite images. *Remote Sensing*, 14(22), 5647. DOI: https://doi.org/10.3390/rs14225647

Bazán, R., Corral, M., Pagot, M., Rodriguez, A., Oroná, C., Rodriguez, M. I., Larrosa, N., Cossavella, A., Del-Olmo, S., Bonfanti, E., & Busso, F. (2005). Teledetección y modelado numérico para el análisis de la calidad de agua del embalse Los Molinos, Córdoba, Argentina. *Ingeniería hidráulica en México*, 20(2), 122-135.

Bramich, J., Bolch, C. J. S., & Fischer, A. (2021). Improved red-edge chlorophyll-a detection for Sentinel-2*. Ecological Indicators*, 120, 106876. DOI: https://doi.org/10.1016/j.ecolind.2020.106876

Caballero, I., & Navarro, G. (2021). Monitoring cyanoHABs and water quality in Laguna Lake (Philippines) with Sentinel-2 satellites during the 2020 Pacific typhoon season. *Science of the Total Environment*, 788, 147700. DOI: https://doi.org/10.1016/j.scitotenv.2021.147700

Chawla, L., Karthikeyan, L., & Mishra, A. K. (2020). A review of remote sensing applications for water security: Quantity, quality, and extremes. *Journal of Hydrology*, 585, 124826. DOI: https://doi.org/10.1016/j.jhydrol.2020.124826

ESA. (2025). *Sentinel-2 user guide*. Retrieved from https://sentinel.esa.int/web/sentinel/user-guides/sentinel-2-msi

GEMS/WATER, Global Environment Monitoring System/Water. (1992). *Operational guide*. Retrieved from https://iris.who.int/bitstream/handle/10665/62446/GEMS_W_92.1(part1).pdf;jsessionid=074E13AFA5FA576FAB3C8EA729C16681?sequence=1

German, A., Shimoni, M., Beltramone, G., & Rodríguez, M. I. (2021). Space-time monitoring of water quality in an eutrophic reservoir using SENTINEL-2 data: A case study of San Roque, Argentina. *Remote Sensing Applications: Society and Environment*, 24 (8), 100614. DOI: https://doi.org/10.1016/j.rsase.2021.100614

Gilabert, M. A., González-Piqueras, J., & García-Haro, J. (1997). Acerca de los índices de vegetación. *Revista de teledetección. Asociación Española de Teledetección*, 8, 1-10. Retrieved from https://www.researchgate.net/publication/39195330

Gilerson, A. A., Gitelson, A. A., Zhou, J., Gurlin, D., Moses, W., Ioannou, I., & Ahmed, S. A. (2010). Algorithms for remote estimation of chlorophyll-a in coastal and inland waters using red and near-infrared bands. *Optics Express*, 18(23), 24109-24125. DOI: https://doi.org/10.1364/OE.18.024109

Gitelson, A. A., & Yacobi, Y. Z. (1995). Reflectance in the red and near-infrared ranges of the spectrum as a tool for remote chlorophyll estimation in inland waters—Lake Kinneret case study. In: *Proceedings of the Eighteenth Convention of Electrical and Electronics Engineers in Israel (IEEE)*. 5.2.6, 1-5. DOI: https://doi.org/10.1109/EEIS.1995.514184

Gitelson, A. A., Dall'Olmo, G., Moses, W., Rundquist, D. C., Barrow, T., Fisher, T. R., Gurlin, D., & Holz, J. (2008). A simple semi-analytical model for remote estimation of chlorophyll-a in turbid waters: Validation. *Remote Sensing of Environment*, 112(9), 3582-3593. DOI: https://doi.org/10.1016/j.rse.2008.04.015

GEE, Google Earth Engine. (2022). *Google Earth Engine: A planetary-scale platform for Earth science data & analysis*. Retrieved from https://earthengine.google.com

Ha, N. T. T., Thao, N. T. P., Koike, K., & Nhuan, M. T. (2017). Selecting the best band ratio to estimate chlorophyll-a concentration in a tropical freshwater lake using Sentinel-2A images: A case study of Lake Ba Be (Northern Vietnam). *ISPRS International Journal of Geo-Information*, 6(9), 290. DOI: https://doi.org/10.3390/ijgi6090290

INA & CIRSA, Instituto Nacional de Agua & Centro de Investigación de la Región Semiárida. (2024). *Informe mensual de monitoreo embalse San Roque*. Córdoba, Argentina: Instituto Nacional de Agua.

Kislik, C., Dronova, I., Grantham, T. E., & Kelly, M. (2022). Mapping algal bloom dynamics in small reservoirs using Sentinel-2 imagery in Google Earth Engine. *Ecological Indicators*, 140, 109041. DOI: https://doi.org/10.1016/j.ecolind.2022.109041

Legates, D. R., & McCabe, G. J. (1999). Evaluating the use of 'goodness-of-fit' measures in hydrologic and hydroclimatic model validation. *Water Resources Research*, 35(1), 233-241. DOI: https://doi.org/10.1029/1998WR900018

Li, P., Hao, F., Wu, H., & Nie, H. (2024). Spatiotemporal dynamic analysis of eutrophication status based on machine learning-based retrieval algorithm: Case study in Liangzi Lake, Hubei, China. *Remote Sensing*, 16(22), 4192. DOI: https://doi.org/10.3390/rs16224192

Li, R., & Li, J. (2004). Satellite remote sensing technology for lake water clarity monitoring: an overview*. Environmental Informatics Archives*, 2, 893-901. Retrieved from https://citeseerx.ist.psu.edu/document?repid=rep1&type=pdf&doi=0bfa92c75e3b3c676af431b21c611a51a8714046

Li, N., Martin, A., & Estival, R. (2017). An automatic water detection approach based on Dempster-Shafer theory for multi spectral images. In: *2017 20th International Conference on Information Fusion (Fusion)* (pp. 1-8). Xi'an, China: Institute of Electrical and Electronics Engineers. DOI: https://doi.org/10.23919/ICIF.2017.8009789

Liu, H., Li, Q., Shi, T., Hu, S., Wu, G. & Zhou, Q. (2017). Application of Sentinel 2 MSI images to retrieve suspended particulate matter concentrations in Poyang Lake. *Remote Sensing*, 9, 761-780. DOI: https://doi.org/10.3390/rs9070761

Maier, P. M., & Keller, S. (2019). Application of different simulated spectral data and machine learning to estimate the chlorophyll-a concentration of several inland waters. In: *10th Workshop on Hyperspectral Imaging and Signal Processing: Evolution in Remote Sensing (WHISPERS)*. Amsterdam, Netherlands: Institute of Electrical and Electronics Engineers (IEEE). DOI: https://doi.org/10.1109/WHISPERS.2019.8921073

Mishra, S., & Mishra, D. R. (2012). Normalized difference chlorophyll index: A novel model for remote estimation of chlorophyll-a concentration in turbid productive waters. *Remote Sensing of Environment*, 117, 394-406. DOI: https://doi.org/10.1016/j.rse.2011.10.016

Muchiut, J., Rodríguez, M. I., Ruibal-Conti, A. L., Ruiz, M., & Rodriguez, A. (2024). Numerical modeling of the influence of reservoir management on the algal blooms of San Roque. *International Journal of Environmental Science and Technology*, 21, 1083-1098. DOI: https://doi.org/10.1007/s13762-023-05102-5

Pagot, M., Rodriguez, A., Hillman, G., Corral, M., & Niencheski, F. (2007). Remote sensing assessment of suspended matter and dynamics in Patos Lagoon. *Journal of Coastal Research*, 47(1), 115-129. DOI: https://doi.org/10.2112/1551-5036-47.sp1.116

Palmer, S. C. J., Hunter, P. D., Lankester, T., Hubbard, S., Spyrakos, E., Tyler, A. N., Présing, M., Horváth, H., Lamb, A., Balzter, H., & Tóth, V. R. (2015). Validation of Envisat MERIS algorithms for chlorophyll retrieval in a large, turbid and optically-complex shallow lake. *Remote Sensing of Environment*, 157, 158-169. DOI: https://doi.org/10.1016/j.rse.2014.07.024

Ponce, G. A., Rodríguez, M. I., Ruibal-Conti, A. L., Muchiut, J., & Rodríguez, A. (2023) Aplicación preliminar del modelo MIKE 21 en un embalse eutrófico durante eventos de crecidas: caso embalse San Roque, Argentina. *Tecnología y ciencias del agua*, 14(3), 314-364. DOI: https://doi.org/10.24850/j-tyca-14-03-07

QGIS.org. (2025). QGIS *Geographic Information System. QGIS Association (3.28.10)*. Retrieved from http://www.qgis.org

Richardson, L. L. (1996). Remote sensing of algal bloom dynamics. *BioScience*, 46(7), 492-501. DOI: https://doi.org/10.2307/1312927

Wackerly, D., Mendenhall III, W., & Scheaffer, R. (2008). *Mathematical statistics with applications* (7th ed.). Belmont, USA: Thomson Brooks/Cole.

Xu, M., Liu, H., Beck, R., Lekki, J., Yang, B., Shu, S., Kang, E. L., Anderson, R., Johansen, R., Emery, E., Reif, M., & Benko, T. (2019). A spectral space partition guided ensemble method for retrieving chlorophyll-a concentration in inland waters from Sentinel-2A satellite imagery. *Journal of Great Lakes Research*, 45(3), 454-465. DOI: https://doi.org/10.1016/j.jglr.2018.09.002

Yu, S., Bai, Y., He, X., Gong, F., & Li, T. (2023). A new merged dataset of global ocean chlorophyll-a concentration for better trend detection. *Frontiers in Marine Science*, (10). DOI: https://doi.org/10.3389/fmars.2023.1051619

Zhang, Q., Yuan, Q., Zeng, C., Li, X., & Wei, Y. (2018). Missing data reconstruction in remote sensing image with a unified spatial-temporal-spectral deep convolutional neural network. *IEEE Transactions on Geoscience and Remote Sensing*, 56 (8), 4274-4288. DOI: https://doi.org/10.1109/TGRS.2018.2810208